

## Effect of spin-orbit coupling on the conduction-electron Zeeman splitting in platinum-group metals

H. Ohlsén

*Department of Solid State Physics, Uppsala University, P.O. Box 534, S-751 21 Uppsala, Sweden*

J. L. Calais

*Department of Quantum Chemistry, Uppsala University, P.O. Box 518, S-751 20 Uppsala, Sweden*

(Received 28 May 1986)

Local  $g$  factors, cyclotron effective masses, and cyclotron-orbit  $g$  factors ( $g_c$ ) for rhodium, palladium, iridium, and platinum have been calculated using a relativistic linear muffin-tin orbital method, including perturbation of a magnetic field. These calculations are compared with experimental results from de Haas–van Alphen measurements. Both measurements and calculations give an anisotropic  $g_c$  factor for the  $\Gamma$ -centered electron sheet and the  $X$  pocket while they give a rather isotropic one for the  $\alpha$  orbit existing on the open-hole sheet. This indicates that the spin-orbit coupling is a major source of the anisotropic behavior of the  $g_c$  factor in these metals.

### I. INTRODUCTION

Experimental results for metals in a magnetic field constitute a real challenge to theoreticians.<sup>1</sup> In particular the amount of Zeeman splitting as measured by the  $g$  factor in general depends on the wave vector and this anisotropy may be influenced by spin-orbit coupling, spin polarization, and probably other factors.

A few theoretical calculations of  $g$  factors in the platinum-group metals exist, both of point  $g$  factors in platinum and palladium calculated by Mueller *et al.*<sup>2</sup> which show a clear  $k$  dependence and of bulk values (see, e.g., MacDonald<sup>3</sup>). From de Haas–van Alphen (dHvA) measurements there is now clear experimental evidence of a large anisotropy of the  $g$  factor on parts of the Fermi surface in the fcc platinum-group metals (rhodium, palladium, iridium, and platinum).<sup>4–8</sup> It is therefore desirable to study this situation also from the theoretical side, first of all, in order to account for the experimental results and hopefully in order to be able to distinguish different reasons for the  $g$ -factor anisotropy. Their Fermi surfaces are well established from dHvA measurements (see, e.g., Carrander *et al.*,<sup>9</sup> Dye *et al.*,<sup>10</sup> Hörnfeldt *et al.*,<sup>11</sup> and Dye *et al.*<sup>12</sup> as well as from band-structure calculations (Mueller *et al.*<sup>13</sup> and Andersen<sup>14</sup>). These metals have the  $\Gamma$ -centered electron sheet ( $\Gamma_6$ ) in common and are therefore well suited for a comparative study. In Refs. 5 and 8 the cyclotron-orbit  $g$  factor ( $g_c$ ) is investigated on the  $\Gamma_6$  sheet and the  $\alpha$  orbit existing near the  $W$  point on the open-hole sheet in palladium and platinum. In Ref. 6 the  $g_c$  factor has been studied on the hole pockets centered around the  $X$  point in palladium and in Refs. 4 and 7 on the  $\Gamma_6$  sheets in rhodium and iridium, respectively. The wave-function character on the open-hole sheet and the  $X_4$  pockets is mainly of  $d$  type, while the  $\Gamma_6$  sheets also have  $s$  and  $p$  character.<sup>14</sup> It is worth noting that the open-hole sheet in palladium and platinum and the  $\Gamma_5$  sheet in rhodium and iridium contributes with more than

half of the total density of states, while the  $X_4$  pockets in palladium and platinum contribute with less than 2%. The calculations presented in this work are concentrated to those parts of the Fermi surface in the fcc platinum-group metals, where dHvA measurements of the  $g_c$  factor have been performed.

Despite the papers just mentioned it cannot be denied that there has been very little done as far as calculations for crystal electrons in a magnetic field is concerned. This is not just by accident. To begin with, there are several basic aspects, in particular concerning symmetry, which are not at all as clearly worked out as in the corresponding problem without a magnetic field. Secondly, there are practical problems connected with the fact that existing procedures and programs have to be extended. In his survey<sup>15</sup> Yafet has characterized the situation in a way which is worth quoting: “To obtain the energy levels of conduction electrons in a magnetic field is a considerably complicated problem.” In Sec. III we discuss some of these problems in a little more detail in order to specify explicitly the theoretical framework for the actual calculations.

Thus there is a lack of balance. There are a number of very good experimental data, but there is definite lack of theoretical studies, which are needed to interpret and explain the experimental results. We have therefore started a series of band calculations including both spin-orbit interaction and a magnetic field. Some technical aspects of these are discussed in Sec. IV. In Sec. V we present the results and compare them with experimental data.

### II. THE $g_c$ FACTOR FROM dHvA MEASUREMENTS

The amplitude of the dHvA signal depends on the  $g_c^*$  factor through a cosine function which arises from a difference in the cross-sectional areas due to the Zeeman splitting into spin-up and spin-down sets of levels at the Fermi level. (Henceforward we use the superscript aster-

isk in order to distinguish between experimentally and theoretically determined quantities.) The argument in the cosine function is  $k\pi R^*$ , where  $k$  is the harmonic number of the dHvA signal and

$$R^* = E_Z/E_L = g_c^* m_c^*/2. \quad (2.1)$$

$E_Z$  is the Zeeman-splitting energy averaged over the cyclotron orbit,  $E_L$  is the Landau level energy spacing, and  $m_c^*$  is the cyclotron effective mass expressed in the free-electron mass. The variation of the  $g_c^*$  factor can be determined from absolute amplitude measurements, from ratios of the harmonics of the dHvA signal or from the locations of field orientations where  $\cos(k\pi R^*)=0$ , that is  $kR^* = n + \frac{1}{2}$  where  $n$  is an integer, which are called spin-splitting zeros (SSZ). These may be found as contours of constant  $R^*$  over the Fermi surface for the different harmonics. A mapping out of the SSZ contours is the most straightforward method and using this together with, for example, the absolute-amplitude method where the experimentally determined amplitude is compared with one calculated from the Lifshitz-Kosevich<sup>16</sup> (LK) theory, the anisotropy of the  $g_c$  factor can be gained. The  $g_c^*$  factor is enlarged by a cyclotron-orbit Stoner enhancement and is unique for each orbit on a specific sheet of the Fermi surface. This is different from the averaged bulk values which can be found through magnetic susceptibility and conduction-electron spin-resonance measurements. Since the  $g_c^*$  factor appears in a cosine function there is an ambiguity in its absolute value. For the transition elements, with a considerable exchange enhancement, a deviation of  $g_c^*$  from two is expected and it is therefore not possible to determine its absolute value. However, the dHvA effect offers a unique possibility to measure its anisotropy.

### III. CRYSTAL ELECTRONS IN A MAGNETIC FIELD

Further information can be obtained from theoretical calculations. At the present state-of-the-art band calculations are more or less routine, provided there are not too many atoms per unit cell, if there is no magnetic field. Relatively few calculations have been carried out, however, with a magnetic field term included in the effective one-electron Hamiltonian. Before getting to the actual calculations in the next section we notice a few important differences between band calculations with and without a magnetic field.

The "normal" situation, which is described in all textbooks, is a crystal with an effective one-electron potential, which takes into account the kinetic energy, the electrostatic interactions with the nuclei and with the other electrons, and—in some average way—exchange and correlation effects. Such a Hamiltonian commutes with all the elements of the space group of the crystal.

When a constant magnetic field is present the situation is a little more complicated. As pointed out by Brown<sup>17</sup> and Zak<sup>18</sup> the translation operators are replaced by a larger set of operators which depend not only on a lattice vector but also on the paths leading from the origin to that vector. These operators form a group, called the

magnetic translation group by Zak. That group must be distinguished from the translation subgroup of a magnetic space group (Shubnikov group).<sup>19</sup>

Thanks to the fact that the magnetic translation group is homomorphic to the usual translation group one can introduce Born—von Kármán conditions in the usual way. Instead of the ordinary Bloch functions which can be factorized in a plane wave and a function which has the periodicity of the direct lattice, one gets a product of a plane wave and two other factors, which depend on the gauge chosen. We will not pursue these aspects any further in the present paper, but we notice the existence of important pieces of information which influence the description of crystal electrons in a magnetic field.

The Dirac equation offers a more natural starting point than the Schrödinger equation for a study of crystal electrons in a magnetic field. An analysis based on that equation has led Moore<sup>20</sup> to a reformulation of the  $g$  factor as a difference of expectation values of the energy operator for wave packets which are well localized in momentum space.

At the simplest level of approximation we can study the influence of two kinds of perturbations on a band Hamiltonian  $H_B$  by means of first-order perturbation theory, namely a Zeeman Hamiltonian

$$H_Z = \mu_B \mathbf{B} \cdot (l + 2s) \quad (3.1)$$

and a Hamiltonian representing the spin-orbit coupling

$$H_{s.o.} = \xi(r) l \cdot s. \quad (3.2)$$

Both these are written in a form appropriate for a free atom, or slightly more generally a system with local spherical symmetry, where one can define an orbital angular momentum  $l$ . In a description of the electronic structure of a crystal, one can still use these forms provided one works with a method which distinguishes spherically symmetric regions around the nuclei, such as the linear muffin-tin orbital (LMTO) method.<sup>21</sup> For symmetry considerations it is however often advantageous to use the more correct form<sup>22</sup>

$$H_{s.o.} = -\frac{i\hbar^2}{2m^2c^2} \mathbf{s} \cdot [\nabla v(r) \times \nabla]. \quad (3.3)$$

Here  $v(r)$  is the periodic crystal potential. We assume that the bands  $E(\mathbf{k})$  for the crystal without spin-orbit coupling and without an external magnetic field are given by the solutions of

$$H_B \psi_\mu(\mathbf{k}, \mathbf{r}) = E_\mu(\mathbf{k}) \psi_\mu(\mathbf{k}, \mathbf{r}). \quad (3.4)$$

An orbitally  $n$ -fold-degenerate level  $E_\mu(\mathbf{k})$ ,  $\mu=1, 2, \dots, n$  gives rise to a  $2n$ -fold degeneracy when spin is taken into account. In spinor notation the corresponding function space is spanned by

$$\begin{aligned} \underline{\phi}_{2\mu-1}(\mathbf{k}, \mathbf{r}) &= \begin{bmatrix} \psi_\mu(\mathbf{k}, \mathbf{r}) \\ 0 \end{bmatrix}, \\ \underline{\phi}_{2\mu}(\mathbf{k}, \mathbf{r}) &= \begin{bmatrix} 0 \\ \psi_\mu(\mathbf{k}, \mathbf{r}) \end{bmatrix}, \end{aligned} \quad (3.5)$$

where  $\mu = 1, 2, \dots, n$ . The spatial part of the Zeeman operator (3.1) is given by

$$h_Z = \int \begin{pmatrix} \alpha \\ \beta \end{pmatrix} H_Z(\alpha\beta) d\xi \\ = \mu_B \mathbf{B} \cdot \mathbf{I} \mathbb{1} + \mu_B \begin{pmatrix} B_z & B_- \\ B_+ & -B_z \end{pmatrix}, \quad (3.6)$$

where  $B_- = B_x - iB_y$ ,  $B_+ = B_x + iB_y$ , and  $\alpha(\xi)$  or  $\beta(\xi)$  are the two spin functions. The first term in this operator in general splits the  $2n$ -fold degeneracy. When both terms of  $h_Z$  are taken into account we get pairs of levels separated by the energy  $2\mu_B B$ . In other words the  $g$  factor is isotropic and independent of  $\mathbf{k}$  and  $\mathbf{B}$ .

When the spin-orbit coupling operator (3.2) is combined with the basic band Hamiltonian  $H_B$  (in the absence of a magnetic field) the symmetry properties of the system are described by the double space group of the crystal.<sup>19,22</sup> The spinors which will be the eigenfunctions of the problem

$$(H_B \mathbb{1} + h_{s.o.}) \underline{\phi}_v(\mathbf{k}, \mathbf{r}) = E_v(\mathbf{k}) \underline{\phi}_v(\mathbf{k}, \mathbf{r}), \quad (3.7)$$

where

$$h_{s.o.} = \int \begin{pmatrix} \alpha \\ \beta \end{pmatrix} H_{s.o.}(\alpha\beta) d\xi \\ = \frac{1}{2} \xi(r) \begin{pmatrix} l_z & l_- \\ l_+ & -l_z \end{pmatrix} \quad (3.8)$$

transform according to the irreducible representations of the double group of the wave vector  $G_0^D(\mathbf{k})$ . A nondegenerate level of the problem (3.4) becomes a doubly degenerate level of (3.7). Degenerate levels of (3.4) may split as a result of the perturbation  $h_{s.o.}$ . A symmetry analysis based on the connection between a space group and its related double space group gives important information as to possible splittings.<sup>22</sup>

If the spinor

$$\underline{\phi}_v(\mathbf{k}, \mathbf{r}) = \begin{pmatrix} \psi_{v1}(\mathbf{k}, \mathbf{r}) \\ \psi_{v2}(\mathbf{k}, \mathbf{r}) \end{pmatrix} \quad (3.9)$$

is a solution of (3.7) with eigenvalue  $E_v(\mathbf{k})$ , so is its time-reversed partner<sup>22</sup>

$$\Theta \underline{\phi}_v(\mathbf{k}, \mathbf{r}) = \begin{pmatrix} -\psi_{v2}^*(\mathbf{k}, \mathbf{r}) \\ \psi_{v1}^*(\mathbf{k}, \mathbf{r}) \end{pmatrix} = \begin{pmatrix} -\psi_{v2}(-\mathbf{k}, \mathbf{r}) \\ \psi_{v1}(-\mathbf{k}, \mathbf{r}) \end{pmatrix}. \quad (3.10)$$

The time-reversal operator is

$$\Theta = -i\sigma_2 K = \begin{pmatrix} 0 & -1 \\ 1 & 0 \end{pmatrix} K. \quad (3.11)$$

This particular degeneracy may be split by the Zeeman operator. We have

$$\langle \Theta \underline{\phi}_v | h_Z | \Theta \underline{\phi}_v \rangle = \mu_B \mathbf{B} [\lambda_{v1}(-\mathbf{k}) + \lambda_{v2}(-\mathbf{k})] \\ + B_z [S_{v22}(-\mathbf{k}) - S_{v11}(-\mathbf{k})] \\ - B_+ S_{v12}(-\mathbf{k}) - B_- S_{v21}(-\mathbf{k}). \quad (3.12)$$

Here

$$\lambda_{vi}(\mathbf{k}) = \int \psi_{vi}^*(\mathbf{k}, \mathbf{r}) I \psi_{vi}(\mathbf{k}, \mathbf{r}) dv, \quad (3.13) \\ S_{vij}(\mathbf{k}) = \int \psi_{vi}^*(\mathbf{k}, \mathbf{r}) \psi_{vj}(\mathbf{k}, \mathbf{r}) dv,$$

where  $i, j = 1, 2$ . Since

$$\lambda_{vi}(-\mathbf{k}) = -\lambda_{vi}(\mathbf{k}), \quad (3.14)$$

and

$$S_{vij}(-\mathbf{k}) = S_{vji}(\mathbf{k}), \quad (3.15)$$

we have

$$\langle \Theta \underline{\phi}_v | h_Z | \Theta \underline{\phi}_v \rangle = -\langle \underline{\phi}_v | h_Z | \underline{\phi}_v \rangle. \quad (3.16)$$

The  $g$  factor,

$$g = g(\mathbf{k}, \mathbf{B}) = \left| \frac{2\langle \Theta \underline{\phi}_v | h_Z | \Theta \underline{\phi}_v \rangle}{\mu_B B} \right|, \quad (3.17)$$

which characterizes this splitting then depends on  $\mathbf{k}$  and we can expect anisotropy both because of the  $\lambda_{vi}(\mathbf{k})$  and the  $S_{vij}(\mathbf{k})$ . Furthermore, the  $g$  factor will exhibit a tensor nature since for a specific  $\mathbf{k}$  different values can be obtained for different directions of the magnetic field.

The Zeeman term (3.6) reduces the symmetry of the system. The final solutions of the full problem

$$(H_B \mathbb{1} + h_{s.o.} + h_Z) \underline{\phi}_v = E_v \underline{\phi}_v, \quad (3.18)$$

transform according to a subgroup of the previously mentioned double space group. Important qualitative results from the dependence of the  $g$  factor of the direction of the magnetic field can be obtained from a detailed symmetry analysis.<sup>23</sup>

In the present paper we have investigated the influence of the spin-orbit and the Zeeman operators on the band structure within a set of basis functions of the linear muffin-tin orbital (LMTO) type.<sup>21</sup> The final energy levels, from which the  $g$  factors are obtained, are the eigenvalues of the full matrix representing the Hamiltonian in (3.18) in the LMTO basis.

#### IV. METHOD OF CALCULATION

The LMTO method in the atomic sphere approximation (ASA) with a muffin-tin potential has been used in order to calculate the cyclotron-orbit-averaged  $g$  factor ( $g_c$ ). The routine was constructed by using the equations given by Skriver in Ref. 21 for the Hamiltonian and overlap matrices. To the Hamiltonian matrix the perturbation from spin-orbit interaction (3.8) (Ref. 24) and from an applied magnetic field  $\mathbf{B}$  (3.6) was added. In order to cut down computing time, orbitals with angular momentum quantum number  $l > 2$  were neglected. To calculate the lattice sums appearing in the structure constants of the LMTO method, the technique outlined by Nijboer and de Wette<sup>25</sup> was used. The routine was constructed in such a way that the structure constants were calculated for each given  $\mathbf{k}$  point, then the Hamiltonian and overlap matrices and finally the eigenvalues for that specific  $\mathbf{k}$  were extracted.

When a magnetic field is applied, only Bloch states on

extremal areas with  $\mathbf{k}$  perpendicular to the magnetic field contribute to the cyclotron orbit. For a given  $\mathbf{B}$  the directions which are perpendicular to the field may be calculated in the crystal coordinate system  $(\theta, \varphi)$ , for any origin. For such a direction  $(\theta, \varphi)$  and for a given band index the length of the  $\mathbf{k}$  vector was changed until the Fermi energy was found within an accuracy of 0.05 mRy and thus giving  $k_F$  in the  $(\theta, \varphi)$  direction and for that specific Fermi-surface sheet. The determination of  $k_F$  was carried out with  $B=0$  T giving a doubly degenerate Fermi energy and once  $k_F$  was found a new calculation was performed with the same  $(\theta, \varphi)$  and  $k_F$  but with  $B=10$  T, thus splitting the degeneracy into  $E^+$  and  $E^-$  energy levels. A local  $g$  factor for a Fermi surface sheet perpendicular to the magnetic field may then be defined as

$$g(\mathbf{k}_F) = (E^+ - E^-) / \mu_B |\mathbf{B}|. \quad (4.1)$$

In order to compare calculations of  $g$  factors with experimental measurements (dHvA) a calculated cyclotron-orbit  $g$  factor ( $g_c$ ) can be related to the local  $g$  factors through a time-weighted average of  $g$  factors at the Fermi surface,  $g(\mathbf{k}_F)$ , which may be written as<sup>26</sup>

$$g_c = \int_{\text{extremal orbit}}^{2\pi} \frac{|\mathbf{k}_F| |g(\mathbf{k}_F) d\varphi'}{\hat{\mathbf{k}}_F \cdot \mathbf{v}_\perp} / \int_{\text{extremal orbit}}^{2\pi} \frac{|\mathbf{k}_F| d\varphi'}{\hat{\mathbf{k}}_F \cdot \mathbf{v}_\perp}, \quad (4.2)$$

where  $\mathbf{v}_\perp$  is the component of  $\mathbf{v} = (1/\hbar)(\nabla_{\mathbf{k}} E)_{\mathbf{k}_F}$  in the plane perpendicular to  $\mathbf{B}$  and the denominator is equal to  $2\pi m_c / \hbar$  expressed in the free electron mass.

The extremal cross-sectional area  $A$  of the specific Fermi-surface sheet, perpendicular to the applied magnetic field, is related to the dHvA frequency  $F$  through the Onsager relation  $F = \hbar A / 2\pi e$  and was calculated from

$$A = \frac{1}{2} \int_{\text{extremal orbit}}^{2\pi} |\mathbf{k}_F|^2 d\varphi'. \quad (4.3)$$

The calculations of the  $g_c$  factor,  $m_c$ , and  $A$  were performed using (4.2) and (4.3), integrating along the cyclotron orbit on the Fermi surface sheet with the Simpson integration technique and  $\Delta\varphi' = 2.5^\circ$ .  $v_\perp$  was calculated for each  $\Delta\varphi'$  using

$$v_\perp = \frac{E(k_F + \Delta k) - E(k_F - \Delta k)}{2\Delta k} \quad (4.4)$$

with  $\Delta k = 10^{-3} 2\pi/a$ , where  $a$  is the lattice constant. The difference in the calculated values of  $A$  compared to the experimentally determined ones were smaller than 10% for all the investigated metals and directions (except for the small  $X$  pockets in platinum). Regarding the difference in  $m_c$ , see Sec. V. Using  $\Delta\varphi' = 1.25^\circ$  changed  $g_c$  less than 0.2% and for  $A$  and  $m_c$  the change was even smaller.

The routine was tested in several ways. With  $B=0$  T the calculated eigenvalues were the same as those calculated using the LMTO routine (including spin-orbit coupling) described in Ref. 21. With  $h_{s.o.} = 0$  the local  $g$  factor was equal to 2 and independent of  $\mathbf{k}$  and  $\mathbf{B}$ . The local  $g$  factor was found to be independent of the magnetic field strength for sufficiently small fields. The symmetry

of  $g_c$  was the same as that for  $A$  and  $m_c$  in the symmetry directions for the  $\Gamma_6$ -centered Fermi-surface sheet, that is fourfold symmetry in the [100] direction, twofold symmetry in the [110] direction, and threefold symmetry in the [111] direction.

The potential parameters, spin-orbit coupling parameters, and Fermi energy for the fcc platinum-group metals were obtained from self-consistent LMTO calculations using the Fortran routine package written by Skriver and described in Ref. 21. The procedure was as follows: fcc structure constants were generated for a mesh of 505  $\mathbf{k}$ -points for  $s$ ,  $p$ , and  $d$  orbitals. The eigenvalues and wave-function character of these  $\mathbf{k}$  points were calculated with a Hamiltonian including spin-orbit interaction. The  $l$ -projected and total state densities plus the  $l$ -projected and total number of states were calculated and together with generated atomic and frozen-core charge densities inserted into the routine which calculates self-consistent potential parameters and ground-state properties. The exchange-correlation potential given by von Barth and Hedin<sup>27</sup> was used. These new potential parameters were then used to calculate new eigenvalues, thus closing the band-iteration loop. The potential parameters in Ref. 21 were taken as starting parameters, i.e., from self-consistent calculations where  $f$  orbitals were included. Only three band iterations were necessary for convergence.

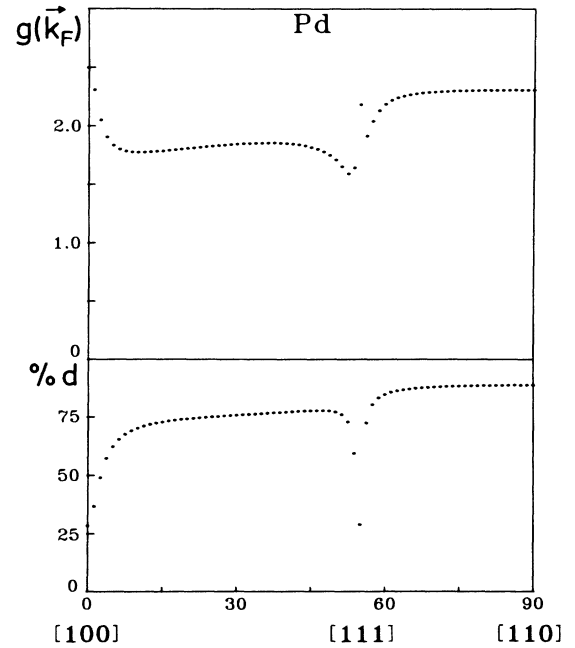


FIG. 1. The local  $g$  factor at the Fermi level  $g(\mathbf{k}_F)$  and percentage  $d$  character of the wave function as a function of angle in a (110) plane on the  $\Gamma_6$  sheet for palladium. The magnetic field is in a [110] direction and perpendicular to the (110) plane.

## V. RESULTS

### A. Local $g(\mathbf{k}_F)$ on the $\Gamma_6$ sheet

With a magnetic field in a [110] direction the cyclotron orbit on the  $\Gamma_6$  sheet passes all the three different types of symmetry directions [100] (two), [110] (two), and [111] (four). The local  $g$  factors  $g(\mathbf{k}_F)$  and the amount of  $d$  character of the wave functions for such an orbit, with  $\mathbf{B}$  parallel to  $[0\bar{1}1]$  ( $\varphi'=0$  to  $\varphi'=\pi/2$ ), are shown in Fig. 1 for palladium and in Fig. 2 for rhodium. A fundamental difference between these metals is the value of  $g(\mathbf{k}_F)$  at [111] with a maximum for palladium while  $g(\mathbf{k}_F)=0$  in rhodium. In iridium and platinum the variation of the local  $g$  factor is similar to that of rhodium.

When studying the band structure in a [111] direction we found for all the fcc platinum-group metals, that the  $g$  factor is equal to zero for two of the  $d$  bands. This is due to symmetry. The double group for  $\Lambda$  points  $C_{3v}^D$  has two one-dimensional irreducible representations  $\Lambda_4$  and  $\Lambda_5$  which are degenerate all the way from  $\Gamma$  to  $L$ . When a magnetic field is applied the symmetry is reduced since only the inversion and the rotations around the field direction commute with the Zeeman Hamiltonian.<sup>23</sup> In a plane perpendicular to the [111] direction there are three (six) directions of the field that "preserve" a twofold rotation from  $C_{3v}^D$ , namely  $\pm[0\bar{1}1]$ ,  $\pm[1\bar{1}0]$ , and  $\pm[10\bar{1}]$ . In these cases the two representations  $\Lambda_4$  and  $\Lambda_5$  will be subduced to two *different* one-dimensional representations of the subgroup,<sup>23</sup> thus preventing any splitting. A more detailed analysis will be given elsewhere. In platinum, rhodium and iridium one of the two  $d$  bands with  $\Lambda_4$  and  $\Lambda_5$  symmetry cuts the Fermi level in such a way that it con-

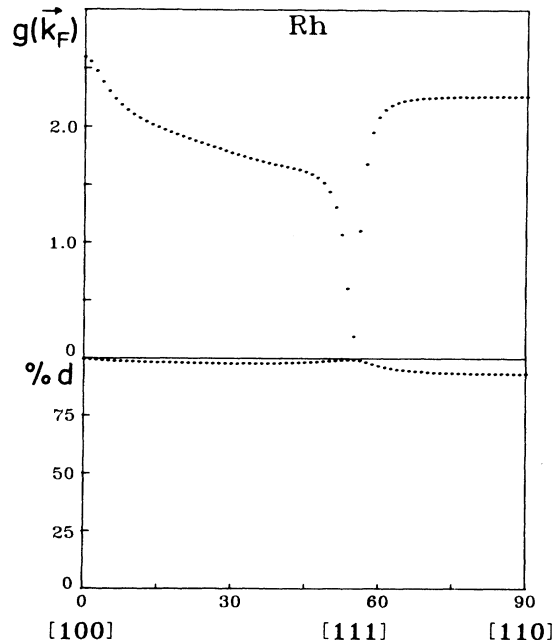


FIG. 2. Same as Fig. 1, but for rhodium.

tributes to the  $\Gamma$ -sheet giving rise to a large  $d$  character in Fig. 2 at [111] and a value  $g(\mathbf{k}_F)=0$ . In palladium, a band with high  $s$ -character crosses the  $d$  band with  $\Lambda_4$  and  $\Lambda_5$  symmetry and cuts the Fermi level (see also Ref. 2) giving rise to a  $g$  factor in the vicinity of 2. The band with  $\Lambda_4$  and  $\Lambda_5$  symmetry in palladium instead contributes to the  $L$  pockets and therefore  $g(\mathbf{k}_F)=0$  in the [111] direction on this part of the Fermi surface in palladium.

### B. Cyclotron effective mass

The cyclotron effective mass ( $m_c^*$ ) has been studied by means of the dHvA technique on the  $\Gamma_6$  sheet,  $\alpha$  orbit, and  $X_4$  pockets in palladium and platinum by Windmiller *et al.*<sup>28</sup> and Ketterson and Windmiller.<sup>29</sup> In Fig. 3 the variation of  $m_c^*$  is presented, which has been determined from the spherical harmonic expansion given in Refs. 28 and 29, in the symmetry planes on the  $\Gamma_6$  sheet in palladium and platinum. When effective masses from theory and experiment are compared, it is normally done by setting  $m_c^*=(1+\lambda)m_c$ , where  $\lambda$  is ascribed to the electron-phonon coupling. In Fig. 3 the calculated  $m_c$  enhanced with  $\lambda=0.43$  for both palladium and platinum are also shown. The largest deviation of 6% occurs at [110] for palladium. Comparison with Refs. 9 and 11 shows that the  $\lambda$  values for the  $\Gamma_6$  sheet seem to be of the same size in rhodium and iridium as in palladium and platinum. For the  $\alpha$  orbit  $\lambda$  is 0.6 for palladium and 0.4 for platinum and for the  $X_4$  pocket the values are 0.9 and 0.8, respectively. The agreement regarding the variation of the effective mass on the  $\Gamma_6$  sheet is good and the electron-phonon interaction can thus be regarded as fairly isotropic in line with results reported previously.<sup>10,12,28,29</sup>

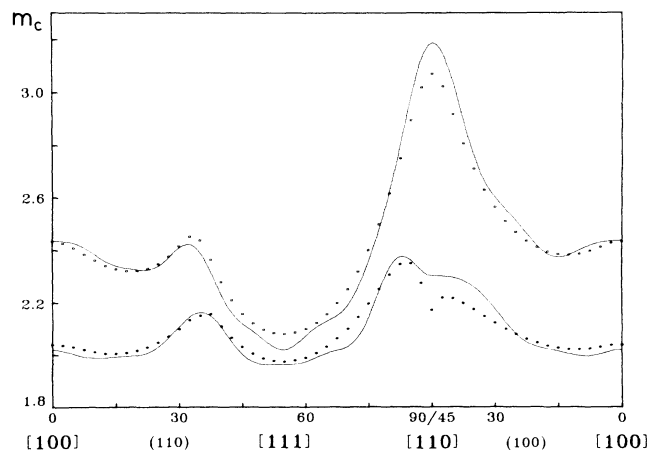


FIG. 3. The calculated cyclotron effective masses, enhanced with a factor 1.43, for palladium ( $\bullet$ ) and platinum ( $\square$ ) in the symmetry planes on the  $\Gamma_6$  sheet. For comparison the measured cyclotron effective masses (weak solid line) are shown for the same metals which were deduced from a spherical harmonic expansion presented in Refs. 28 and 29.

### C. Cyclotron-orbit $g$ factors

In Fig. 4 the calculated  $g_c$  factors in the symmetry planes on the  $\Gamma_6$  sheets in palladium, platinum, rhodium, and iridium are presented as functions of the direction of the magnetic field. The main feature for all the fcc platinum-group metals is a large dip in the graphs at [110] while a smaller dip occurs at  $35^\circ$  from [100] in the (110) plane. It is for these directions of the magnetic field that the cyclotron-orbit passes the [111] directions. With the magnetic field in the [110] direction four [111] directions are passed, while for the field in the direction of  $35^\circ$  from [100] in the (110) plane two [111] directions are passed. It therefore seems that the major contribution to the anisotropy of the  $g_c$  factor comes from the anisotropy of the local  $g$  factors in the region near [111]. The behavior of the  $g_c$  factor in palladium and rhodium is very similar, with somewhat larger dips in rhodium than in palladium. The variation of the  $g_c$  factor is much larger for platinum and iridium. The value of the  $g_c$  factor at [100] and  $35^\circ$  out in the (110) plane are nearly equal for platinum and iridium but when comparing the difference between the maximum at [111] and the minimum at [110] this is much larger for platinum than for iridium. Both palladium and platinum have a maximum at  $15^\circ$  from [100] in the (110) plane but it is more pronounced in

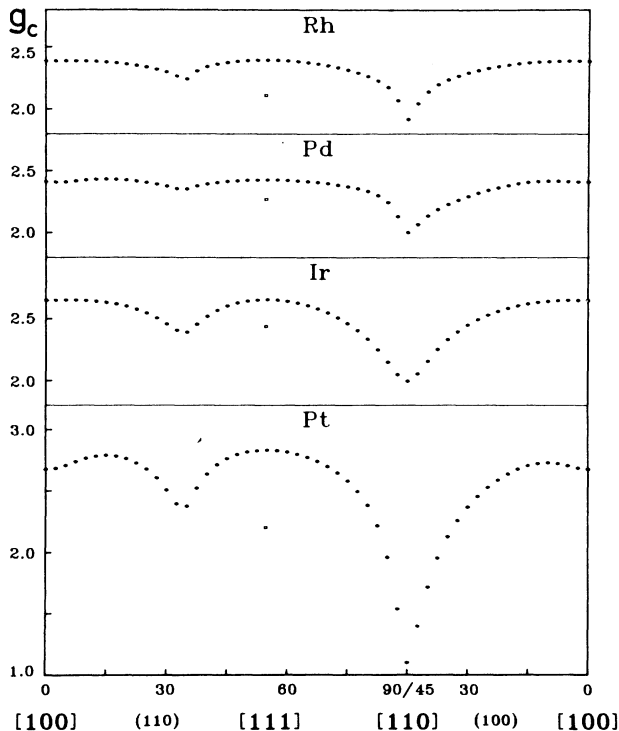


FIG. 4. The calculated  $g_c$  factor in the symmetry planes on the  $\Gamma_6$  sheet in palladium, platinum, rhodium, and iridium (●). The  $g_c$  factor for the noncenter orbit at [111] is also shown (□).

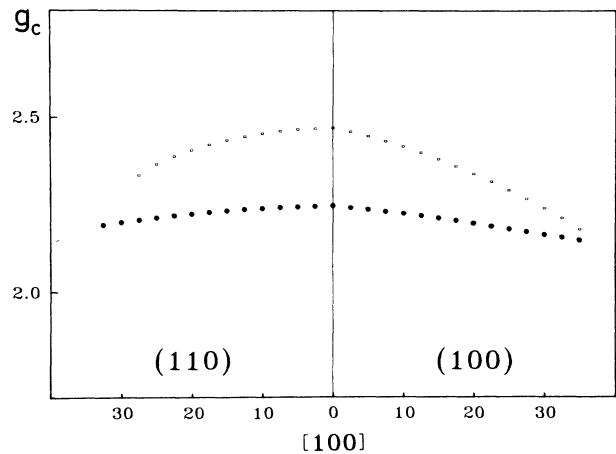


FIG. 5. The calculated  $g_c$  factor in the symmetry planes for the  $\alpha$  orbit in palladium (●) and platinum (□).

platinum than in palladium. The gross features of the anisotropy of the  $g_c$  factor are rather similar to the experimental data presented in Refs. 5 and 8 but there are some differences. For platinum, the variation of  $g_c^*$  near [100] and [110] does not show up in the calculations and for palladium the maximum at [111] is more pronounced for  $g_c^*$ . The latter difference may, however, be due to hidden SSZ contours in the area where the central orbit splits off into one center and two noncenter orbits (for details see Ref. 5) which could lead to a somewhat different picture for the  $g_c^*$  factor. Calculations have also been performed for the noncenter orbit at [111] and its  $g_c$ -factor value is shown in Fig. 4 for the different metals. An experimentally determined variation of  $g_c^*$  for the noncenter orbit has only been presented for palladium and platinum.<sup>5,8</sup> Both the theoretical and experimental values for the noncenter orbit are smaller than those for the center orbit at [111].

In Fig. 5 the calculated  $g_c$  factor for the  $\alpha$  orbit in the symmetry planes is presented (it only exists in palladium and platinum). In contrast to the anisotropic behavior on the  $\Gamma_6$  sheet the  $g_c$  factor is here clearly isotropic. This has also been shown to be the case experimentally.

In Fig. 6 the calculated  $g_c$  factors for the ellipsoidally shaped  $X_4$  pockets in palladium and platinum are shown. The large variation on this small part of the Fermi surface with nearly pure  $d$  character is surprising but this was also shown experimentally in Refs. 6, 30, and 31 to be the case for palladium. The two maxima of the  $g_c$  factor occurring at approximately  $20^\circ$  from the "belly" of the ellipsoid are more pronounced in palladium than in platinum. Noticeable are the low values ( $<0.7$ ) for the entire  $X_4$  pocket in platinum and the low value at [001] for both palladium and platinum. The  $X_4$  pocket for platinum has been examined experimentally to some extent by Cavalloni *et al.*<sup>31</sup> Their measurements are not in contradiction to the theoretical values presented in this work.

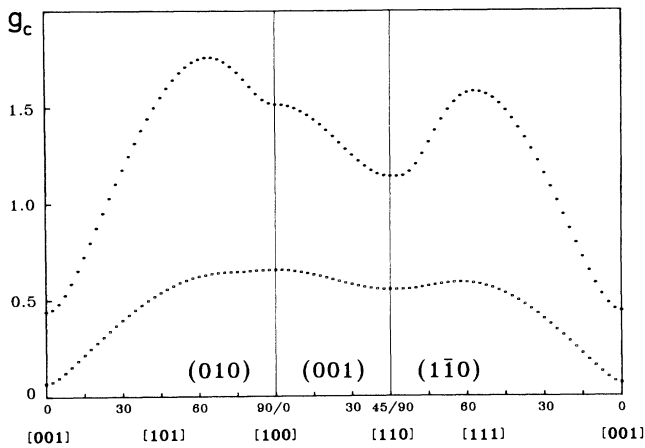


FIG. 6. The calculated  $g_c$  factor in the symmetry planes for the  $X$  pockets situated at  $[001]$  in palladium (●) and platinum (□).

## VI. DISCUSSION AND CONCLUSIONS

The primary purpose of the present investigation was to study to what extent band theory can account for the experimentally observed anisotropy of the  $g$  factors in the platinum-group metals. The main result is that this does indeed seem to be the case, but this statement needs to be qualified. Band theory normally means *effective* one-electron theory in the sense that many-body effects are taken into account in some kind of average way, and despite impressive advances in density functional theory it is somewhat of a mystery that it works so well. Apart from that basic problem we also have here all the complications connected with the external magnetic field. Even if in principle we stand at the band theory level there are a number of practical aspects connected with the particular procedure used and various approximations associated with it. Qualitative, and to a certain extent quantitative agreement, has been achieved between theory and experiment but there is definitely room for improvement:

(i) The  $f$  orbitals have been neglected in the present study and the basis set should be extended to also include these.

(ii) Effects of spin polarization might have an influence on the  $g$  factor and should be studied.

It must also be remembered that:

(a) The cyclotron-orbit Stoner factor is expected to influence the experimentally determined  $g_c^*$  factors and may account for some of the differences when comparing theory and experiment.

(b) Landau condensation is not included in band theory, but is believed to be of minor importance when comparing theoretical calculations to experimental measurements.

If one compares the difference between the maximum and minimum values of the measured  $R^*$  ( $\Delta R^*$ ) with the maximum and minimum values of the calculated  $R$  ( $\Delta R$ ) one must also in some way take into account the Stoner enhancement and using the experimentally determined

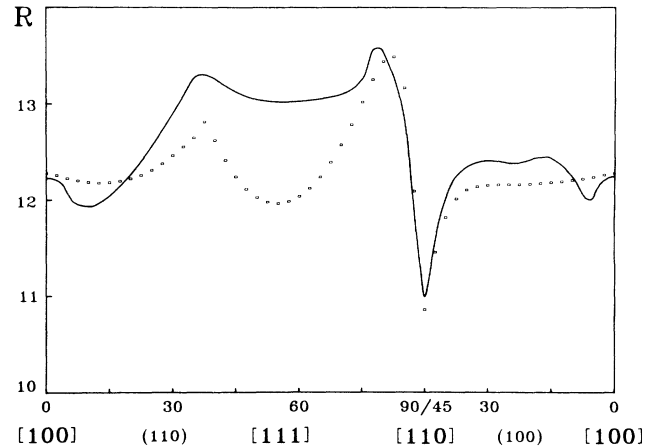


FIG. 7. The calculated values of  $R$  on the  $\Gamma_6$  sheet in palladium, enhanced with a factor 7.1, and the measured  $R^*$  (solid line) with the integer part of  $R^*$  equal to 12.

bulk values ( $S$ ): for palladium  $\Gamma_6$ :  $\Delta R^* = 2.6$ ,  $S = 7.6$ ,<sup>5</sup>  $\Delta R = 0.4$ ; palladium  $X_4$ :  $\Delta R^* = 1.7$ ,  $S = 7.6$ ,<sup>5</sup>  $\Delta R = 0.5$ ; iridium  $\Gamma_6$ :  $\Delta R^* \leq 0.7$ ,  $S = 1.3$ ,<sup>7</sup>  $\Delta R = 0.5$ ; platinum  $\Gamma_6$ :  $\Delta R^* = 1.5$ ,  $S = 3.1$ ,<sup>8</sup>  $\Delta R = 1.1$ . For rhodium enough data are not yet available but an anisotropy in  $R^*$  has been observed.<sup>4</sup> From the data above it is clear that it is not a correct approach to simply multiply  $\Delta R$  with  $S$  to achieve  $\Delta R^*$ . Some possibilities emerge:

The cyclotron-orbit Stoner enhancement is anisotropic in such a way that  $RS$  shows less anisotropy as compared to the case with an isotropic  $S$ .

The Stoner enhancement is smaller for the  $\Gamma_6$  sheet and the  $X_4$  pockets.

The anisotropy due to spin-orbit coupling will not be enhanced in the same way as its average bulk value.

In Fig. 7 a comparison between the theoretical  $R$  and experimental  $R^*$  (Ref. 5) of palladium is presented in the symmetry planes. All the  $R$  values have been multiplied with a factor of 7 in order to give the same value of  $\Delta R$  as  $\Delta R^*$ . The experimental curve for  $R^*$  from Ref. 5 was plotted with the integer part of  $R^*$  equal to 12.

Previously there have been very few theoretical works in this field and the present work must be seen as a first step in an investigation of cyclotron-orbit  $g$  factors in metals. It is shown that the behavior of the measured  $g_c^*$  factor which is anisotropic on the  $\Gamma_6$  sheet and the  $X_4$  pockets while it is isotropic on the  $\alpha$  orbit, can be explained by the spin-orbit interaction.

## ACKNOWLEDGMENTS

The LMTO routine package provided by Dr. Hans Skriver has played an essential role in the present paper. The assistance offered by M. Sc. Olle Eriksson for using it in Uppsala is gratefully acknowledged. We are indebted to Dr. Peter Gustafsson and Dr. Lars Nordborg for valuable discussions. This work has been supported by the Swedish Natural Science Research Council.

- <sup>1</sup>See, e.g., J. C. Slater, *Quantum Theory of Molecules and Solids* (McGraw-Hill, New York, 1967), Vol. III.
- <sup>2</sup>F. M. Mueller, A. J. Freeman, and D. D. Koelling, *J. Appl. Phys.* **41**, 1229 (1970).
- <sup>3</sup>A. H. MacDonald, *J. Phys. F* **12**, 2579 (1982).
- <sup>4</sup>H. Ohlsén, P. Gustafsson, and L. Nordborg, *J. Phys. F* **16**, L79 (1986).
- <sup>5</sup>H. Ohlsén, P. Gustafsson, L. Nordberg, and S. P. Hörnfeldt, *Phys. Rev. B* **29**, 3022 (1984).
- <sup>6</sup>H. Ohlsén, P. Gustafsson, and L. Nordborg, *J. Phys. F* **16**, 1681 (1986).
- <sup>7</sup>P. Gustafsson, H. Ohlsén, and L. Nordborg (unpublished).
- <sup>8</sup>P. Gustafsson, H. Ohlsén, and L. Nordborg, *Phys. Rev. B* **33**, 3749 (1986).
- <sup>9</sup>K. Carrander, M. Dronjak, and S. P. Hörnfeldt, *J. Phys. Chem. Solids* **38**, 289 (1977).
- <sup>10</sup>D. H. Dye, S. A. Campbell, G. W. Crabtree, J. B. Ketterson, N. B. Sandesara, and J. J. Vuillemin, *Phys. Rev. B* **23**, 462 (1981).
- <sup>11</sup>S. P. Hörnfeldt, L. R. Windmiller, and J. B. Ketterson, *Phys. Rev. B* **7**, 4349 (1973).
- <sup>12</sup>D. H. Dye, J. B. Ketterson, and G. W. Crabtree, *J. Low Temp. Phys.* **30**, 813 (1978).
- <sup>13</sup>F. M. Mueller, A. J. Freeman, J. O. Dimmock, and A. M. Furdyna, *Phys. Rev. B* **1**, 4817 (1970).
- <sup>14</sup>O. K. Anderson, *Phys. Rev. B* **2**, 883 (1970).
- <sup>15</sup>Y. Yafet, *Solid State Phys.* **14**, 1 (1963).
- <sup>16</sup>I. M. Lifshitz and A. M. Kosevich, *Zh. Eksp. Teor. Fiz.* **29**, 730 (1955) [*Sov Phys.—JETP* **2**, 636 (1956)].
- <sup>17</sup>E. Brown, *Phys. Rev.* **133**, A1038 (1964); *Solid State Phys.* **22**, 313 (1968).
- <sup>18</sup>J. Zak, *Phys. Rev.* **134**, A1602 (1964); **134**, A1607 (1964).
- <sup>19</sup>C. J. Bradley and A. P. Cracknell, *The Mathematical Theory of Symmetry in Solids* (Clarendon, Oxford, 1972).
- <sup>20</sup>R. A. Moore, *J. Phys. F* **5**, 459 (1975).
- <sup>21</sup>H. Skriver, *The LMTO Method* (Springer-Verlag, Berlin, 1984).
- <sup>22</sup>J. F. Cornwell, *Group Theory and Electronic Energy Bands in Solids* (North-Holland, Amsterdam, 1969).
- <sup>23</sup>L. M. Falicov and J. Ruvalds, *Phys. Rev.* **172**, 498 (1968).
- <sup>24</sup>O. K. Anderson, *Band Structure of Transition Metals*, Mont Tremblant International Summer School, 1973 (unpublished).
- <sup>25</sup>B. R. A. Nijboer and F. W. de Wette, *Physica* **23**, 309 (1957).
- <sup>26</sup>P. M. Holtham, *Can. J. Phys.* **51**, 368 (1973).
- <sup>27</sup>U. von Barth and L. Hedin, *J. Phys. C* **5**, 1629 (1972).
- <sup>28</sup>L. R. Windmiller, J. B. Ketterson, and S. P. Hörnfeldt, *Phys. Rev. B* **3**, 4213 (1971).
- <sup>29</sup>J. B. Ketterson and L. R. Windmiller, *Phys. Rev. B* **2**, 4813 (1970).
- <sup>30</sup>P. T. Coleridge, P. Wise, P. Reinders, and M. Springford (private communication).
- <sup>31</sup>C. Cavalloni, W. Joss, R. Monnier, and T. Jarlborg, *Phys. Rev. B* **31**, 1744 (1985).